



TITLE:

Theoretical Studies of Translational Nonequilibrium and Velocity Slip in a Freejet Expansion of a Binary Gas Mixture

AUTHOR(S):

TAKAHASHI, Norio; TESHIMA, Koji

CITATION:

TAKAHASHI, Norio ...[et al]. Theoretical Studies of Translational Nonequilibrium and Velocity Slip in a Freejet Expansion of a Binary Gas Mixture. *Memoirs of the Faculty of Engineering, Kyoto University* 1983, 45(3): 79-98

ISSUE DATE:

1983-11-30

URL:

<http://hdl.handle.net/2433/281250>

RIGHT:

Theoretical Studies of Translational Non-equilibrium and Velocity Slip in a Freejet Expansion of a Binary Gas Mixture

By

Norio TAKAHASHI* and Koji TESHIMA*

(Received March 31, 1983)

Abstract

Parallel temperature of each species and velocity slip in a freejet of a binary rare gas mixture are numerically solved by using an ellipsoidal velocity distribution function, the moment method of the Boltzmann equation and by assuming the flow as a spherically symmetrical one. An attractive part of the Lennard-Jones (12, 6) potential is used as an intermolecular potential model. In order to simplify the calculation of collision terms between light and heavy species, an equal perpendicular temperature for each species and a very small velocity slip are assumed. It is obtained that the frozen parallel temperature of the heavy species is higher than that of the light species. Also, the ratio of their frozen parallel temperatures and the terminal velocity slip increase by increasing the mass ratio and by decreasing the mole fraction of the heavy species.

1. Introduction

The kinetic energy of a molecular beam is fixed by a reservoir temperature: an energy of 65 meV is obtained from a room temperature reservoir for a monatomic gas. For a higher energy beam, a reservoir-heating method, an acceleration of a heavy species by a light carrier gas (the seeded beam method)¹⁾ or their coupled method²⁾ are generally used. The seeded beam method is the useful one to obtain the beam in a wide range of energy by changing the concentration and the mass ratio. However, the expansion is so rapid that the collision numbers are not enough to keep an isentropic expansion at a few times orifice-diameter distance downstream from an orifice, so that non-equilibrium phenomena as mass separation, velocity slip and translational non-equilibrium occur.¹⁻⁵⁾ Theoretical treatments for the velocity slip and translational non-equilibrium have been made by Miller and Andres,⁵⁾ Willis and Hamel,⁶⁾ Cooper and Bienkowski,⁷⁾ and Soga and Oguchi.⁸⁾ They have solved this flow problem by the

* Department of Aeronautical Engineering

moment method of the Boltzmann equation, assuming the flow as a spherically symmetrical expansion. Willis and Hamel, and Soga and Oguchi have used the BGK model, and have predicted that the frozen temperature of a heavy species is lower than that of a light species. However, Miller and Andres, and Cooper and Bienkowski have evaluated the collision terms more realistically, and gave predictions opposite to those of Willis and Hamel, and Soga and Oguchi. Recently, Chatwani and Fiebig⁹⁾ have calculated the same problem by the direct Monte-Carlo simulation method and obtained that the frozen temperature of a heavy species is higher than that of a light species. On the other hand, experimental studies¹⁻⁵⁾ have shown results similar to Miller and Andres' calculation, Cooper and Bienkowski's theory and Chatwani and Fiebig's Monte-Carlo result. These opposite predictions about the translational non-equilibrium between light and heavy species make the understanding of the translational relaxation process of the binary mixture confused, which has motivated us to make an another theoretical approach. We assume a freejet expansion as a spherically symmetrical one and a velocity distribution function of each species as an ellipsoidal one. We then solve the moment equation of the Boltzmann equation numerically. This model has been already applied by Miller and Andres,⁶⁾ Knuth and Fisher,¹⁰⁾ and Toennies and Winkelmann¹¹⁾ to analyze the translational non-equilibrium in a freejet expansion of a pure rare gas, and could explain the experimental results very well.^{5,12,13)} Although deviations from the Maxwellian distributions cannot be considered in this model, we can directly evaluate collision terms using a realistic inter-molecular potential model. In order to obtain simplified equations for the collision terms between light and heavy species, we introduce two assumptions: (a) the perpendicular temperature is equal for each species, and (b) the velocity slip is much smaller than the stream velocities. Hence, the present calculated results show that the frozen temperature of a heavy species is higher than that of a light species in accordance with the theoretical predictions of Miller and Andres,⁶⁾ Cooper and Bienkowski,⁷⁾ and Chatwani and Fiebig⁹⁾, and also with previous experimental observations.¹⁻⁵⁾

2. Fundamental Equations

Basic assumptions of the present theory are that the expansion downstream from an orifice is a spherically symmetrical flow and that a velocity distribution of gas molecules of species i , $f_i(\mathbf{V}_i)$, obeys an ellipsoidal one given by

$$f_i(\mathbf{V}_i) = n_i \left(\frac{m_i}{2\pi k T_{\parallel i}} \right)^{\frac{1}{2}} \left(\frac{m_i}{2\pi k T_{\perp i}} \right)^{\frac{1}{2}} \exp \left[-\frac{m_i}{2k T_{\parallel i}} (v_{\parallel i} - u_i)^2 - \frac{m_i}{2k T_{\perp i}} v_{\perp i}^2 \right], \quad (2.1)$$

where $v_{\parallel i}$ and $v_{\perp i}$ are respectively the parallel and perpendicular velocity components of velocity, \mathbf{V}_i , with respect to a streamline, $T_{\parallel i}$ and $T_{\perp i}$ the corresponding translational temperatures, n_i is the number density, u_i the stream velocity, m_i the mass and k the

Boltzmann constant. In the following discussions, we denote subscripts 1 and 2 as light and heavy species, respectively.

With the ellipsoidal velocity distribution function, the Boltzmann equation in spherical coordinates can be written by

$$\frac{\partial}{\partial r} v_{\parallel i} f_i - \frac{m_i}{r k T_{\parallel i}} (v_{\parallel i} - u_i) v_{\perp i}^2 f_i + \frac{m_i v_{\parallel i} v_{\perp i}^2}{k T_{\perp i}} f_i = \sum_{j=1}^2 \left(\frac{\partial f_i}{\partial t} \right)_{coll, i, j}, \quad (2.2)$$

where $(\partial f_i / \partial t)_{coll, i, j}$ describes the change of f_i due to the self- or cross-collision. The moment method is used to obtain the fundamental equations for four different functions of velocity components, i. e., m_i , $m_i v_{\parallel i}$, $m_i (v_{\parallel i}^2 + v_{\perp i}^2) / 2$ and $m_i v_{\perp i}^2 / 2$. The results are summarized in Table I, where $\Delta_{ij}[\Phi(V_i)]$ is called the collision term between species i and j on some arbitrary function of velocity components, $\Phi(V_i)$. According to the parallel momentum and the total energy conservation principles during a collision, the following conservation equations on collision terms are obtained:

$$\Delta_{12}[m_1 v_{\parallel 1}] + \Delta_{21}[m_2 v_{\parallel 2}] = 0, \quad (2.3)$$

$$\Delta_{12}\left[\frac{m_1}{2}(v_{\parallel 1}^2 + v_{\perp 1}^2)\right] + \Delta_{21}\left[\frac{m_2}{2}(v_{\parallel 2}^2 + v_{\perp 2}^2)\right] = 0. \quad (2.4)$$

Equations (I) – (IV) in Table I are rearranged and normalized by using the following reduced parameters:

$$r^* = \frac{r}{d}, \quad n_i^* = \frac{n_i}{n_{0i}}, \quad T_i^* = \frac{T_i}{T_0}, \quad u_i^* = \frac{u_i}{u_{maxi}}, \quad (2.5)$$

Table I. Fundamental set of moment equations of the Boltzmann equation using ellipsoidal velocity distribution function.

Physical meaning	$\Phi(V_i)$	Resulting momentum equations	
Conservation of mass for species i	m_i	$\frac{d}{dr}(m_i n_i u_i r^2) = 0,$	(I)
Equation of parallel momentum for species i	$m_i v_{\parallel i}$	$n_i u_i \frac{d}{dr} m_i u_i + \frac{1}{r^2} \frac{d}{dr} r^2 n_i k T_{\parallel i} - \frac{2 n_i k T_{\perp i}}{r}$ $= \Delta_{ii}[m_i v_{\parallel i}],$	(II)
Equation of total energy for species i	$\frac{1}{2} m_i (v_{\parallel i}^2 + v_{\perp i}^2)$	$n_i u_i \frac{d}{dr} \left(\frac{3}{2} k T_{\parallel i} + \frac{m_i}{2} u_i^2 \right) + n_i u_i \frac{d}{dr} k T_{\perp i}$ $= \Delta_{ii} \left[\frac{m_i}{2} (v_{\parallel i}^2 + v_{\perp i}^2) \right],$	(III)
Equation of perpendicular energy for species i	$\frac{1}{2} m_i v_{\perp i}^2$	$n_i u_i \frac{d}{dr} k T_{\perp i} + \frac{2 n_i u_i k T_{\perp i}}{r}$ $= \Delta_{ii} \left[\frac{m_i}{2} v_{\perp i}^2 \right] + \Delta_{ij} \left[\frac{m_i}{2} v_{\perp i}^2 \right],$	(IV)
where		$\Delta_{ij}[\Phi(V_i)] = \int_{-\infty}^{\infty} \Phi(V_i) \left(\frac{\partial f_i}{\partial t} \right)_{coll, i, j} dV_i.$	(V)

where n_{0i} is the density of species i at the reservoir, T_0 its temperature, d the orifice diameter and u_{maxi} the maximum stream velocity obtained by a pure gas expansion of species i , and is given by $u_{maxi} = (5kT_0/m_i)^{1/2}$. Then, we obtain the following reduced equations:

$$n_i^* u_i^* r^{*2} = F_i, \quad (2.6)$$

$$\left(\frac{1}{2} - \frac{3T_{\perp i}^*}{10u_i^{*2}} \right) \frac{du_i^*}{dr^*} = \frac{T_{\perp i}^*}{5u_i^* r^*} + \frac{3}{10u_i^*} \mathcal{C}_{1i} + \frac{1}{5u_i^*} \mathcal{C}_{2i}, \quad (2.7)$$

$$\left(\frac{1}{2} - \frac{3T_{\parallel i}^*}{10u_i^{*2}} \right) \frac{dT_{\parallel i}^*}{dr^*} = - \left(1 - \frac{T_{\parallel i}^*}{5u_i^{*2}} \right) \mathcal{C}_{2i} - \mathcal{C}_{1i} - \frac{2T_{\parallel i}^* T_{\perp i}^*}{5r^* u_i^{*2}}, \quad (2.8)$$

$$\frac{dT_{\perp i}^*}{dr^*} = - \frac{2T_{\perp i}^*}{r^*} + \mathcal{C}_{3i}, \quad (2.9)$$

$$\mathcal{C}_{1i} = \frac{m_i d}{n_{0i} k T_0} \cdot \frac{1}{n_i^*} \cdot \mathcal{A}_{ij}[v_{\parallel i}], \quad (2.10)$$

$$\mathcal{C}_{2i} = \frac{m_i d}{2n_{0i} k T_0 u_{maxi}} \cdot \frac{1}{n_i^* u_i^*} (\mathcal{A}_{ii}[v_{\perp i}^2] - \mathcal{A}_{ij}[v_{\parallel i}^2]), \quad (2.11)$$

$$\mathcal{C}_{3i} = \frac{m_i d}{2n_{0i} k T_0 u_{maxi}} \cdot \frac{1}{n_i^* u_i^*} (\mathcal{A}_{ii}[v_{\perp i}^2] + \mathcal{A}_{ij}[v_{\perp j}^2]), \quad (2.12)$$

where F_i is the reduced flux of the flow for species i and is constant during the expansion. In order to solve Eqs. (2.6)-(2.9), all the collision terms must be determined at each step of the numerical integration. Using the conservation relations, we need calculate only $\mathcal{A}_{ii}[v_{\perp i}^2]$, $\mathcal{A}_{ij}[v_{\parallel i}]$, $\mathcal{A}_{ij}[v_{\perp i}^2]$, $\mathcal{A}_{ij}[v_{\parallel i}^2]$, $\mathcal{A}_{ji}[v_{\perp j}^2]$ and $\mathcal{A}_{jj}[v_{\perp j}^2]$ of all the collision terms, and can determine $\mathcal{A}_{ji}[v_{\parallel j}]$ and $\mathcal{A}_{ji}[v_{\parallel j}^2]$ from Eqs. (2.3) and (2.4). However, because these calculations include the sixth-order multiple integrals, except for $\mathcal{A}_{ii}[v_{\perp i}^2]$ and $\mathcal{A}_{jj}[v_{\perp j}^2]$, simplification of these calculations is made in the next section.

3. Evaluation of Collision Terms

3.1 Collision terms between different species

A collision term on an elastic binary collision between species i and j is given by¹⁴⁾

$$\mathcal{A}_{ij}[\Phi(V_i)] = \int_{-\infty}^{\infty} \int_{-\infty}^{\infty} \int_0^{4\pi} \delta\Phi(V_i) f_i(V_i) f_j(C_j) g \sigma_{ij} d\Omega dC_j dV_i, \quad (3.1)$$

where V_i is the velocity for species i , C_j that for species j , σ_{ij} the collision cross section between species i and j , g the relative velocity, $\delta\Phi(V_i) = \Phi(V_i') - \Phi(V_i)$, and the prime denotes the state after a collision. We calculate Eq. (3.1) for $\Phi(V_i) = v_{\parallel i}$, $v_{\parallel i}^2$, $v_{\perp i}^2$ and $v_{\perp i}^2$ using the ellipsoidal velocity distribution function for each species. Furthermore, in order to simplify the equations of the collision terms, we introduce the assumption that the perpendicular temperature may be always equal for each species during the expansion, that is, $T_{\perp 1} = T_{\perp 2} = T_{\perp}$. Then, the order of multiple integrals is

reduced to four from six, and the following equations are obtained:

$$\mathcal{A}_{12}[v_{\parallel 1}] = 4 \frac{m_2}{M} B \int_0^\infty \int_{-1}^1 \int_0^\infty \int_{-1}^1 g^4 W^2 n Q_{12}^{(D)} H d\xi dW d\eta dg, \quad (3.2)$$

$$\mathcal{A}_{12}[v_{\perp 1}^2] = 2 \left(\frac{m_2}{M} \right)^2 B \int_0^\infty \int_{-1}^1 \int_0^\infty \int_{-1}^1 (3\eta^2 - 1) g^5 W^2 Q_{12}^{(D)} H d\xi dW d\eta dg, \quad (3.3)$$

$$\begin{aligned} \mathcal{A}_{12}[v_{\parallel 1}^2] &= -\mathcal{A}_{12}[v_{\perp 1}^2] - 2u_1 \mathcal{A}_{12}[v_{\parallel 1}] \\ &+ 8 \frac{m_2}{M} B \int_0^\infty \int_{-1}^1 \int_0^\infty \int_{-1}^1 W^3 g^4 \xi \eta Q_{12}^{(D)} H d\xi dW d\eta dg, \end{aligned} \quad (3.4)$$

$$\mathcal{A}_{21}[v_{\perp 2}^2] = -\left(\frac{m_1}{m_2} \right)^2 \mathcal{A}_{12}[v_{\perp 1}^2], \quad (3.5)$$

where

$$B = n_1 n_2 (\beta_{\parallel 1} \beta_{\parallel 2})^{1/2} (\beta_{\perp 1} \beta_{\perp 2}) / \pi, \quad (3.6)$$

$$\begin{aligned} H = \exp \left[-\frac{MW^2}{2kT_{w\text{eff}12}} - \frac{\mu_{12}g^2}{2kT_{s\text{eff}12}} - 2gW\xi\eta \left(\beta_{\parallel 2} \frac{m_1}{M} - \beta_{\parallel 1} \frac{m_2}{M} \right) \right. \\ \left. - 2\beta_{\perp 2} \Delta u \left(W\xi + \frac{m_1}{M} g\eta \right) - \beta_{\perp 2} (\Delta u)^2 \right], \end{aligned} \quad (3.7)$$

$$T_{w\text{eff}12}^{-1} = \frac{1}{M} \left(\frac{m_1}{T_{\parallel 1}} + \frac{m_2}{T_{\parallel 2}} \right) \xi^2 + \frac{1 - \xi^2}{T_{\perp}}, \quad (3.8)$$

$$T_{s\text{eff}12}^{-1} = \frac{1}{M} \left(\frac{m_1}{T_{\parallel 2}} + \frac{m_2}{T_{\parallel 1}} \right) \eta^2 + \frac{1 - \eta^2}{T_{\perp}}. \quad (3.9)$$

In the reduction of Eqs. (3.2)–(3.9), two transformations of the velocity coordinates system have been made. One is the transformation to the center of mass (c. m.) system (W_k, g_k) from the Lab. one (v_{1k}, v_{2k}), and the other is that to the spherical coordinates system ($W, \phi_w, \theta_w, g, \phi_g, \theta_g$) from the rectangular one. The relations between these velocity components are given by

$$v_{1k} = W_k - \frac{m_2}{M} g_k, \quad v_{2k} = W_k + \frac{m_1}{M} g_k, \quad (3.10)$$

$$\begin{aligned} W_1 - u_1 &= W \cos \phi_w, & g_1 &= g \cos \phi_g, \\ W_2 &= W \sin \phi_w \cos \theta_w, & g_2 &= g \sin \phi_g \cos \theta_g, \\ W_3 &= W \sin \phi_w \sin \theta_w, & g_3 &= g \sin \phi_g \sin \theta_g, \end{aligned} \quad (3.11)$$

where W is the c. m. velocity, ϕ the angle between W or g and the parallel direction, and θ the azimuthal angle between the plane including W or g and some arbitrary reference plane including the parallel axis. In Eq. (3.2)–(3.9), Δu is the velocity slip and is defined by $\Delta u = u_1 - u_2$, μ_{12} the reduced mass, $\beta_i = m_i / 2kT_i$, $\xi = \cos \phi_w$, $\eta = \cos \phi_g$, $M = m_1 + m_2$, $Q_{12}^{(D)}$ and $Q_{12}^{(V)}$ are respectively the diffusion and viscosity collision cross sections, and $T_{w\text{eff}12}$ and $T_{s\text{eff}12}$ the effective temperatures related to the c. m. velocity and the relative velocity. In Eq. (3.7), the third factor of the exponential denotes the translational non-equilibrium effect between species i and j , and the fourth and

fifth factors denote the velocity slip effect. The assumption of the equal perpendicular temperature for each species is made because of the prediction that a perpendicular temperature would keep an isentropic expansion during the expansion from the calculated results for the freejets of pure gases.¹¹ With this assumption, the order of the fundamental equations is reduced to seven from eight, and the following relation on collision terms is obtained from Eq. (2, 9):

$$\frac{m_1}{n_1 u_1} (\mathcal{A}_{11}[v_{1_1}^2] + \mathcal{A}_{12}[v_{1_1}^2]) = \frac{m_2}{n_2 u_2} (\mathcal{A}_{21}[v_{1_2}^2] + \mathcal{A}_{22}[v_{1_2}^2]). \quad (3.12)$$

This relation means that the summation of the collision terms on the perpendicular energy between light-light and light-heavy species is determined from that between heavy-light and heavy-heavy species and vice versa. The evaluation of the collision cross section between species i and j needs an inter-molecular potential model. In the present calculation, the Lennard-Jones (12, 6) potential is used and is given by

$$V_{ij}(R) = \epsilon_{ij} [(Rm_{ij}/R)^{12} - 2(Rm_{ij}/R)^6],$$

where R is the inter-nuclear distance, ϵ_{ij} the well depth of the potential and Rm_{ij} its location. In the case of a classical treatment, as discussed by Hirschfelder et. al.^{15,16} and Toennies and Winkelmann,¹¹ the collision cross section at the small reduced collision energies ($E/\epsilon_{ij} < 0.7$) is approximately given by

$$Q_{ij}^{(0)} \cong A_6^{(0)} 2\pi \left(\frac{6C_{6ij}}{E} \right)^{1/3}, \quad (3.13)$$

where $E = \mu_{ij} g^2/2$, $C_{6ij} = 2\epsilon_{ij} Rm_{ij}^6$, $A_6^{(1)} = 0.306$ and $A_6^{(2)} = 0.331$. Potential parameters used in the present calculation are shown in Table II.

Introducing the assumption of the equal perpendicular temperatures, we can simplify the collision terms including the sixth-order multiple integrals to those including the fourth-order ones. In order to further simplify these calculations, we introduce the

Table II. Well depth ϵ and its location Rm for Lennard-Jones (12, 6) potential model.^{a)}

System	ϵ (meV)	Rm (Å)
He-He	0.91	2.99
Ne-Ne	3.78	3.09
Ar-Ar	12.46	3.74
Kr-Kr	16.40	4.03
He-Ne [†]	1.89	3.01
He-Ar	2.20	3.55
He-Kr	2.13	3.75

a) Reference 17.

assumption that the velocity slip is much smaller than the stream velocities, and expand the collision terms in powers of the velocity slip with the truncation of its second or fourth and higher order terms in the next paragraph.

(a) First-order approximation of velocity slip

In the first-order approximation of the velocity slip, the fourth and fifth factors of the exponential in Eq. (3.7)

are expressed by

$$\exp\left[-2\beta_{n_2}\Delta u\left(W\xi + \frac{m_1}{M}g\eta\right) - \beta_{n_1}(\Delta u)^2\right] \cong 1 - 2\beta_{n_2}\Delta u\left(W\xi + \frac{m_1}{M}g\eta\right). \quad (3.14)$$

Substituting Eq. (3.14) for Eqs. (3.2)-(3.4), we expand the third factor in Eq. (3.7) into a power series as follows:

$$\exp\left[-2gW\xi\eta\left(\beta_{n_2}\frac{m_1}{M} - \beta_{n_1}\frac{m_2}{M}\right)\right] = \sum_{l=0}^{\infty} \frac{(-1)^l}{l!} \left[2gW\xi\eta\left(\beta_{n_2}\frac{m_1}{M} - \beta_{n_1}\frac{m_2}{M}\right)\right]^l.$$

Introducing the following reduced parameters:

$$\omega^2 = \frac{MW^2}{2kT_{\text{eff}12}}, \quad \gamma^2 = \frac{\mu_{12}g^2}{2kT_{\text{eff}12}},$$

we can replace the fourth-order multiple integral in the collision terms with an infinite series of multiplications of four single integrals on ξ , η , ω and γ . Further, the single integrals on ω and γ can be presented with known analytic functions. Then, in the first-order approximation of the velocity slip we obtain

$$\begin{aligned} \mathcal{A}_{12}[v_{n_1}]_{\text{first}} &= 4\left(\frac{2kT_0}{m_1}\right)\left(10\pi\frac{m_2}{M}\right)^{\dagger} A_6^{(3)}\left(\frac{6C_{612}}{kT_0}\right)^{\dagger} \frac{n_1n_2}{(T_{n_1}^*T_{n_2}^*)^{\dagger}T_{\perp}^{*2}} \\ &\quad \times \left(\frac{\Delta u^*}{T_{n_2}^*}\right)\left[\left(\frac{m_2}{M}\right)\text{SUM } 1 - \text{SUM } 2\right], \end{aligned} \quad (3.15)$$

$$\mathcal{A}_{12}[v_{\perp 1}^2]_{\text{first}} = 2\left(\frac{2kT_0}{m_1}\right)^{\dagger}\left(\pi\frac{m_2}{M}\right)^{\dagger} A_6^{(3)}\left(\frac{6C_{612}}{kT_0}\right)^{\dagger} \frac{n_1n_2}{(T_{n_1}^*T_{n_2}^*)^{\dagger}T_{\perp}^{*2}} \text{SUM } 3, \quad (3.16)$$

$$\begin{aligned} \mathcal{A}_{12}[v_{n_1}^2]_{\text{first}} &= -\mathcal{A}_{12}[v_{\perp 1}^2]_{\text{first}} - 2u_1\mathcal{A}_{12}[v_{n_1}]_{\text{first}} - 8\left(\frac{2kT_0}{M}\right)^{\dagger} \\ &\quad \times \left(\pi\frac{m_2}{m_1}\right)^{\dagger} A_6^{(3)}\left(\frac{6C_{612}}{kT_0}\right)^{\dagger} \frac{n_1n_2}{(T_{n_1}^*T_{n_2}^*)^{\dagger}T_{\perp}^{*2}} \text{SUM } 1, \end{aligned} \quad (3.17)$$

where

$$\text{SUM } 1 = \sum_{i=0}^{\infty} \frac{(2i+3)!!}{(2i+1)!} 2^i K^{2i+1} \left(\frac{\mu_{12}}{M}\right)^i \Gamma\left(\frac{8}{3} + i\right) FG(i) FW(i+1), \quad (3.18)$$

$$\text{SUM } \left\{ \begin{matrix} 2 \\ 3 \end{matrix} \right\} = \sum_{j=0}^{\infty} \frac{(2j+1)!!}{(2j)!} 2^j K^{2j} \left(\frac{\mu_{12}}{M}\right)^j \Gamma\left(\frac{8}{3} + j\right) \left\{ \begin{matrix} FG(j) \\ FI(j) \end{matrix} \right\} FW(j), \quad (3.19)$$

$$FW(k) = \int_0^1 T_{\text{Weff}12}^{*{\dagger}+k} \xi^{2k} d\xi \quad (3.20)$$

$$FG(k) = \int_0^1 T_{\text{seff}12}^{*{\dagger}+k} \eta^{2(1+k)} d\eta, \quad (3.21)$$

$$FI(k) = \int_0^1 T_{\text{seff}12}^{*{\dagger}+k} \eta^{2k} (3\eta^2 - 1) d\eta, \quad (3.22)$$

where $l=2j$ or $2i+1$, $\Delta u^* = \Delta u/u_{\text{max}}$, $\Gamma(n)$ is the gamma function of n -th order and $K = (1/T_{n_2}^* - 1/T_{n_1}^*)$. Because $T_{\text{Weff}12}$ is the even function of ξ and $T_{\text{seff}12}$ is the even

function on γ , the zero-order term of velocity slip in $\mathcal{A}_{12}[v_{\parallel 1}]$ and the first-order term in $\mathcal{A}_{12}[v_{\perp 1}^2]$ are identically equal to zero, and thus the effect of the velocity slip is included only in $\mathcal{A}_{12}[v_{\parallel 1}]$ and $\mathcal{A}_{12}[v_{\perp 1}^2]$ for the first-order approximation of the velocity slip. In order to determine the collision terms, we need only to integrate $\mathbf{FW}(k)$, $\mathbf{FG}(k)$ and $\mathbf{FI}(k)$ numerically, and to sum up Eqs. (3. 18) and (3. 19) until converging, respectively.

(b) Third-order approximation of velocity slip

In the third-order approximation of the velocity slip, the fourth and fifth factors in Eq. (3. 7) are expressed by

$$\begin{aligned} \exp\left[-2\beta_{\parallel 2}\Delta u\left(W\xi + \frac{m_1}{M}g\eta\right) - \beta_{\perp 2}(\Delta u)^2\right] &\cong [1 - \beta_{\parallel 2}(\Delta u)^2] \left[1 - 2\beta_{\perp 2}\Delta u\left(W\xi + \frac{m_1}{M}g\eta\right)\right] \\ &+ \frac{2^2}{2!}\beta_{\perp 2}^2(\Delta u)^2\left(W\xi + \frac{m_1}{M}g\eta\right)^2 - \frac{2^3}{3!}\beta_{\perp 2}^3(\Delta u)^3\left(W\xi + \frac{m_1}{M}g\eta\right)^3. \end{aligned} \quad (3. 23)$$

Equation (3. 23) is substituted for Eqs. (3. 2)-(3. 4), and in the same way as described in the previous paragraph, the collision terms in the third-order approximation of the velocity slip are obtained as follows:

$$\begin{aligned} \mathcal{A}_{12}[v_{\parallel 1}]_{\text{third}} &= \left[1 - \frac{5}{2}\left(\frac{m_2}{m_1}\right)\left(\frac{\Delta u^{*2}}{T_{\perp 2}^*}\right)\right]\mathcal{A}_{12}[v_{\parallel 1}]_{\text{first}} + 8\sqrt{\pi}\left(\frac{2kT_0}{m_1}\right)\left(\frac{5m_2}{2M}\right)^{\dagger}A_6^{(1)} \\ &\times \left(\frac{6C_{612}}{kT_0}\right)^{\dagger} \frac{n_1n_2}{(T_{\parallel 1}^*T_{\perp 2}^*)^{1/2}T_{\perp 1}^{*2}}\left(\frac{\Delta u^*}{T_{\perp 2}^*}\right)^3 \left[\frac{1}{3}\cdot\text{SUM 4} - \text{SUM 5} + 2\cdot\text{SUM 6} - \frac{2}{3}\cdot\text{SUM 7}\right], \end{aligned} \quad (3. 24)$$

$$\begin{aligned} \mathcal{A}_{12}[v_{\perp 1}^2]_{\text{third}} &= \left[1 - \frac{5}{2}\left(\frac{m_2}{m_1}\right)\left(\frac{\Delta u^{*2}}{T_{\perp 2}^*}\right)\right]\mathcal{A}_{12}[v_{\perp 1}^2]_{\text{first}} + 5\sqrt{\pi}\left(\frac{2kT_0}{M}\right)^{\dagger}\left(\frac{m_2}{m_1}\right)^{\dagger}A_6^{(2)} \\ &\times \left(\frac{6C_{612}}{kT_0}\right)^{\dagger} \frac{n_1n_2}{(T_{\parallel 1}^*T_{\perp 2}^*)^{1/2}T_{\perp 1}^{*2}}\left(\frac{\Delta u^*}{T_{\perp 2}^*}\right)^2 [\text{SUM 8} - 4\cdot\text{SUM 9} + \left(\frac{M}{m_1}\right)^{\dagger}\text{SUM 10}], \end{aligned} \quad (3. 25)$$

$$\begin{aligned} (\mathcal{A}_{12}[v_{\parallel 1}^2] + \mathcal{A}_{12}[v_{\perp 1}^2] + 2u_1\mathcal{A}_{12}[v_{\parallel 1}])_{\text{third}} &= \left[1 + \frac{5}{2}\left(\frac{m_2}{m_1}\right)\left(\frac{\Delta u^{*2}}{T_{\perp 2}^*}\right)\right] \\ &\times (\mathcal{A}_{12}[v_{\parallel 1}^2] + \mathcal{A}_{12}[v_{\perp 1}^2] + 2u_1\mathcal{A}_{12}[v_{\parallel 1}])_{\text{first}} - 20\sqrt{\pi}\left(\frac{2kT_0}{M}\right)^{\dagger}\left(\frac{m_2}{m_1}\right)^{\dagger} \\ &\times A_6^{(1)}\left(\frac{6C_{612}}{kT_0}\right)^{\dagger} \frac{n_1n_2}{(T_{\parallel 1}^*T_{\perp 2}^*)^{1/2}T_{\perp 1}^{*2}}\left(\frac{\Delta u^*}{T_{\perp 2}^*}\right)^2 [\text{SUM 4} - 2\cdot\text{SUM 5} + 2\cdot\text{SUM 6}], \end{aligned} \quad (3. 26)$$

where

$$\text{SUM 4} = \left(\frac{m_2}{M}\right)\left(\frac{m_2}{m_1}\right)\sum_{i=0}^{\infty}\frac{(2i+5)!!}{(2i+1)!}2^iK^{2i+1}\left(\frac{\mu_{12}}{M}\right)^i\Gamma\left(\frac{8}{3}+i\right)\mathbf{FG}(i)\mathbf{FW}(i+2), \quad (3. 27)$$

$$\text{SUM}\left\{\begin{matrix} 5 \\ 10 \end{matrix}\right\} = \left(\frac{m_2}{m_1}\right)\sum_{j=0}^{\infty}\frac{(2j+3)!!}{(2j)!}2^jK^{2j}\left(\frac{\mu_{12}}{M}\right)^j\Gamma\left(\frac{8}{3}+j\right)\left\{\begin{matrix} \mathbf{FG}(j) \\ \mathbf{FI}(j) \end{matrix}\right\}\mathbf{FW}(j+1), \quad (3. 28)$$

$$SUM\left\{\begin{matrix} 6 \\ 9 \end{matrix}\right\} = \left(\frac{m_2}{M}\right) \sum_{i=0}^{\infty} \frac{(2i+3)!!}{(2i+1)!} 2^i K^{2i+1} \left(\frac{\mu_{12}}{M}\right)^i \Gamma\left(\frac{11}{3}+i\right) \left\{\begin{matrix} FG(i+1) \\ FI(i+1) \end{matrix}\right\} FW(i+1), \quad (3.29)$$

$$SUM\left\{\begin{matrix} 7 \\ 8 \end{matrix}\right\} = \sum_{j=0}^{\infty} \frac{(2j+1)!!}{(2j)!} 2^j K^{2j} \left(\frac{\mu_{12}}{M}\right)^j \Gamma\left(\frac{11}{3}+j\right) \left\{\begin{matrix} FG(j+1) \\ FI(j+1) \end{matrix}\right\} FW(j). \quad (3.30)$$

The nomenclature is the same as that used in the previous paragraph. The second-order term of the velocity slip in Eq. (3.24) and the third-order terms in Eq. (3.25) and (3.26) are identically equal to zero. If $FW(k)$, $FG(k)$ and $FI(k)$ are once calculated to determine the collision terms for the first-order approximation of the velocity slip at each step of the numerical integration, we can also determine the collision terms for the third-order approximation.

3.2 Collision term between same species

A collision term on an elastic binary collision between same species i is given by¹⁰

$$A_{ii}[\Phi(V_i)] = \int_{-\infty}^{\infty} \int_{-\infty}^{\infty} \int_0^{4\pi} [\delta\Phi(V_i) + \delta\Phi(C_i)] f_i(V_i) f_i(C_i) g \sigma_{ii} d\Omega dC_i dV_i. \quad (3.31)$$

We calculate Eq. (3.31) for $\Phi(V_i) = v_{\perp i}^2$, together with Eqs. (2.1) and (3.13), and obtain a much simpler equation than those for the collision terms between different species as follows:

$$A_{ii}[v_{\perp i}^2] = \left(\frac{\pi}{2}\right)^{\dagger} \left(\frac{2kT_0}{m_i}\right)^{\dagger} A_6^{\infty} \left(\frac{6C_{6ii}}{kT_0}\right)^{\dagger} \frac{n_i^{\dagger}}{T_{ii}^{\dagger} T_{\perp i}^{\dagger}} \Gamma\left(\frac{8}{3}\right) \times \int_0^1 T_{eff ii}^{\dagger} (3\eta^2 - 1) d\eta, \quad (3.32)$$

where $T_{eff ii}^{\dagger} = \eta^2/T_{ii}^{\dagger} + (1-\eta^2)/T_{\perp i}^{\dagger}$. Equation (3.32) is the same as that obtained by Toennies and Winkelmann.¹¹

On the assumption of the equal perpendicular temperatures we need only to calculate one of the collision terms between the light-light and heavy-heavy species because the other is determined from Eq. (3.12). Since the mole fraction of the heavy species is usually very small in the seeded beam method, we calculate the collision term between the light-light species, $A_{11}[v_{\perp 1}^2]$, from Eq. (3.32) and determine $A_{22}[v_{\perp 2}^2]$ from Eq. (3.12). However, we predict that the difference between $A_{22}[v_{\perp 2}^2]$ determined from Eq. (3.12) and that calculated from Eq. (3.32) may not be small. Thus, its effect on the calculated results may become large with an increase of the mole fraction of the heavy species. In order to include the collision term on the perpendicular energy between the heavy-heavy species in the calculation correctly, we also calculate $A_{22}[v_{\perp 2}^2]$ from Eq. (3.32) by neglecting the relation of Eq. (3.12). Even in this case, neglecting the non-equilibrium effect on the perpendicular tempe-

perature in the calculation of the collision terms between different species, we use an effective perpendicular temperature defined by

$$T_{\perp,eff} = \chi_1 T_{\perp 1} + \chi_2 T_{\perp 2}, \quad (3.33)$$

where χ_i is the mole fraction of species i .

4. Calculation Method

The set of Eqs. (2.6)–(2.9) is numerically solved together with Eqs. (2.3) and (2.4) to get the quantities n_i^* , n_2^* , u_1^* , u_2^* , $T_{\parallel 1}^*$, $T_{\parallel 2}^*$ and $T_{\perp 1}^*$ or $T_{\perp 1}^*$ and $T_{\perp 2}^*$ with the Runge–Kutta–Gill method. Because the assumption of the equal perpendicular temperatures is introduced, Eq. (2.9) is applied to $T_{\perp}^*(=T_{\perp 1}^*=T_{\perp 2}^*)$ and the relation of Eq. (3.12) is added. Meanwhile, in the case of using Eq. (3.33), Eq. (2.9) is solved for both i and j species. The collision terms between different species are calculated from Eqs. (3.5) and (3.15)–(3.17) for the first-order approximation of the velocity slip, and Eqs. (3.5) and (3.24)–(3.26) for the third-order approximation of the velocity slip. Since the first term in the left-hand side of Eq. (2.9) describes the geometrical term and contributes greatly to the cooling process of the translational temperatures, we can use the criterion that each increment of \mathcal{C}_{11} , \mathcal{C}_{21} and \mathcal{C}_{31} in Eqs. (2.7)–(2.9) becomes infinitesimal compared with the geometrical term, $(-2T_{\perp 1}^*/r^*)$, as the convergence condition of the collision terms between different species at the location r^* . On the other hand, the collision terms between same species are calculated from Eqs. (3.12) and (3.32) in the case of $T_{\perp 1}^*=T_{\perp 2}^*=T_{\perp}^*$, or only from Eq. (3.32) in the case of using Eq. (3.33).

The initial conditions are determined by the Ashkenas and Sherman formula¹⁶⁾ at some distance downstream from the orifice in the range of $r^*=1.2-1.8$, assuming that the expansion is isentropic to the starting point. The numerical calculation is terminated when the ratio of the perpendicular temperature to the parallel temperature of the light species becomes less than 0.05.

5. Results and Discussions

The dependencies of the frozen parallel temperature of each species and the velocity slip on the convergence condition for the collision terms between different species calculated at $P_0 d = 7$ Torr·cm and $T_0 = 300$ K for 98% He–2% Ar and 97% He–3% Ar mixtures for the first-order approximation of the velocity slip are shown in Table III. It can be seen that the calculated results are weakly depending on the convergence condition and become constant for a condition less than 10^{-6} . In the following calculations, we used the value of 10^{-7} as the convergence condition.

Typical results of perpendicular and parallel temperature changes during the

Table III. Dependency of calculated results on convergence condition for collision terms.

Convergence condition	$P_0 d$ Torr·cm	T_0 K	χ_2 %	$T_{ 1}^\infty$ K	$T_{ 2}^\infty$ K	S_{T1}^∞	S_{T2}^∞	$\Delta u^\infty / u_{1, \text{max}}$ %
10^{-1}	7	300	2	3.0908	11.832	14.337	22.569	2.5021
10^{-2}	7	300	2	3.0910	11.898	14.336	22.510	2.4883
10^{-3}	7	300	2	3.1049	11.288	14.303	23.116	2.4559
10^{-4}	7	300	2	3.1047	11.218	14.303	23.188	2.4538
10^{-5}	7	300	2	3.0936	11.197	14.329	23.211	2.4530
10^{-6}	7	300	2	3.0936	11.196	14.329	23.211	2.4530
10^{-7}	7	300	2	3.0936	11.196	14.329	23.211	2.4530
10^{-1}	7	300	3	2.9645	10.636	14.133	23.006	2.4136
10^{-2}	7	300	3	2.9585	10.559	14.147	23.092	2.3887
10^{-3}	7	300	3	2.9699	10.176	14.119	23.526	2.3716
10^{-4}	7	300	3	2.9699	10.135	14.119	23.574	2.3704
10^{-5}	7	300	3	2.9699	10.131	14.119	23.578	2.3704
10^{-6}	7	300	3	2.9699	10.131	14.119	23.579	2.3704
10^{-7}	7	300	3	2.9699	10.131	14.119	23.579	2.3704

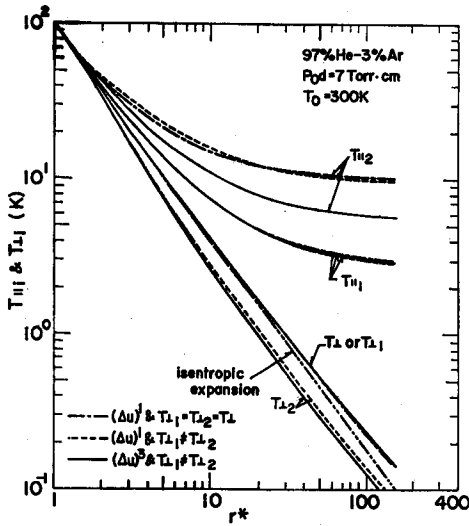


Fig. 1. Parallel and perpendicular temperature changes during the expansion of a 97% He-3% Ar mixture calculated at $P_0 d = 7$ Torr·cm and $T_0 = 300$ K for three cases: (i) $T_{||1} = T_{||2} = T_{\perp}$ using the $(\Delta u)^1$ approximation, (ii) $T_{||1} \neq T_{||2}$ using $(\Delta u)^1$ and (iii) $T_{||1} \neq T_{||2}$ using $(\Delta u)^3$.

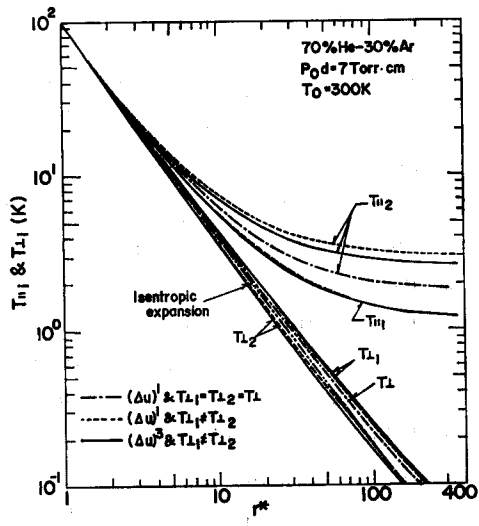


Fig. 2. Parallel and perpendicular temperature changes during the expansion of a 70% He-30% Ar mixture calculated at $P_0 d = 7$ Torr·cm and $T_0 = 300$ K for three cases.

expansion of 97% He-3% Ar and 70% He-30% Ar mixtures calculated at $P_0d=7$ Torr·cm and $T_0=300$ K are respectively shown in Figs. 1 and 2 for three cases: the summation of $\mathcal{A}_{22}[v_{\perp 2}^2]$ and $\mathcal{A}_{21}[v_{\perp 2}^2]$ is determined from Eq. (3.12) using the first-order approximation of the velocity slip terms [the case of $T_{\perp 1}=T_{\perp 2}=T_{\perp}$ using the $(\Delta u)^1$ approximation], that is calculated from Eqs. (3.5) and (3.32) using the first-order approximation [the case of $T_{\perp 1}\neq T_{\perp 2}$ using $(\Delta u)^1$] and using the third-order approximation [the case of $T_{\perp 1}\neq T_{\perp 2}$ using $(\Delta u)^3$]. It can be seen that the parallel temperature of the heavy species always becomes higher than that of the light species during the expansion for all cases. For the case of $T_{\perp 1}=T_{\perp 2}=T_{\perp}$, the rate of the change of T_{\perp} becomes gradually smaller than that of the isentropic expansion with r^* . For the case of $T_{\perp 1}\neq T_{\perp 2}$, the perpendicular temperature of the heavy species becomes lower than that of the light species with r^* : the temperature change of $T_{\perp 1}$ almost agrees with that of T_{\perp} , while the rate of the change of $T_{\perp 2}$ becomes larger than that of the isentropic expansion with an increase of r^* and a decrease of the mole fraction of the heavy species, χ_2 . On the other hand, $T_{\parallel 1}$ shows no apparent dependency on the assumption of the equal perpendicular temperatures and the approximation of the velocity slip, but $T_{\parallel 2}$ shows a prominent dependency on them. In Fig. 1, $T_{\parallel 2}$ calculated for $T_{\perp 1}=T_{\perp 2}=T_{\perp}$ using $(\Delta u)^1$ is almost equal to that for $T_{\perp 1}\neq T_{\perp 2}$ using $(\Delta u)^1$, but is much higher than that for $T_{\perp 1}\neq T_{\perp 2}$ using $(\Delta u)^3$. In Fig. 2, $T_{\parallel 2}$ calculated for $T_{\perp 1}\neq T_{\perp 2}$ using $(\Delta u)^1$ is much higher than that for $T_{\perp 1}=T_{\perp 2}=T_{\perp}$ using $(\Delta u)^1$, but is close to that for $T_{\perp 1}\neq T_{\perp 2}$ using $(\Delta u)^3$. The difference between the change of $T_{\parallel 2}$ for the $(\Delta u)^1$ approximation and that for $(\Delta u)^3$ in Fig. 1 is due to the truncation error of the velocity slip in the calculation of the collision terms, and the difference between the change of $T_{\parallel 2}$ for $T_{\perp 1}=T_{\perp 2}=T_{\perp}$, and that for $T_{\perp 1}\neq T_{\perp 2}$ in Fig. 2 is due to the difference between the summation of $\mathcal{A}_{22}[v_{\perp 2}^2]$ and $\mathcal{A}_{21}[v_{\perp 2}^2]$ determined from Eq. (3.12) and that calculated from Eqs. (3.5) and (3.32). From these results, we can know that the assumption of the equal perpendicular temperatures is invalid, but has only a weak effect on the result for $T_{\parallel 2}$ in the small range of χ_2 and further, it has no effect on the result for $T_{\parallel 1}$. On the other hand, the truncation error of the velocity slip in the calculation of the collision terms has a prominent effect on the result for $T_{\parallel 2}$ in the small range of χ_2 , but no apparent effect on that for $T_{\parallel 1}$.

Dependencies of a frozen parallel temperature, $T_{\parallel i}^{\infty}$, a terminal speed ratio defined by $S_{\parallel i}^{\infty}=(m_i u_i^{\infty}/2kT_{\parallel i}^{\infty})^{1/2}$, and a terminal velocity slip defined by $\Delta u^{\infty}=(u_1^{\infty}-u_2^{\infty})/u_{i, \text{max}}$ on the mole fraction of the heavy species calculated at $P_0d=7$ Torr·cm and $T_0=300$ K are shown in Figs. 3-5 for the He-Ne, He-Ar and He-Kr mixtures, respectively, where $u_{i, \text{max}}$ is the maximum stream velocity achieved from the isentropic expansion of the mixture. It can be seen that the frozen parallel temperature of the heavy species

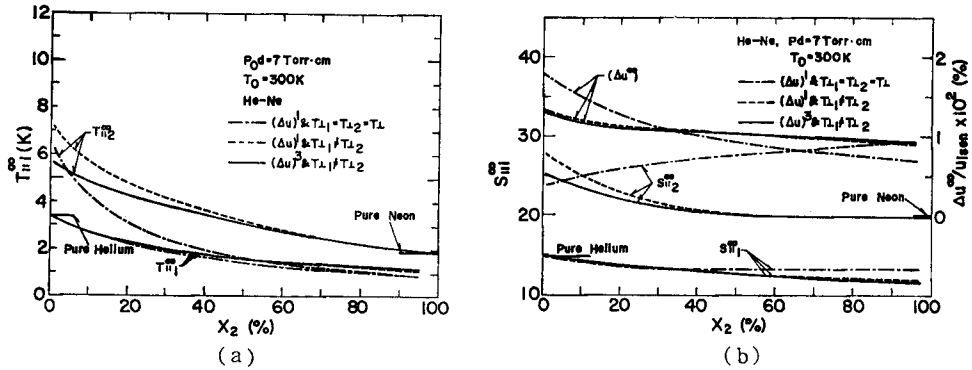


Fig. 3. Dependencies of (a) frozen parallel temperature of each species, (b) terminal speed ratio of each species and terminal velocity slip on mole fraction of heavy species, χ_2 , for an He-Ne mixture calculated at $P_0 d = 7$ Torr·cm and $T_0 = 300$ K for three cases: (i) $T_{L1} = T_{L2} = T_L$ using the $(\Delta u)^1$ approximation, (ii) $T_{L1} \neq T_{L2}$ using $(\Delta u)^1$ and (iii) $T_{L1} \neq T_{L2}$ using $(\Delta u)^3$.

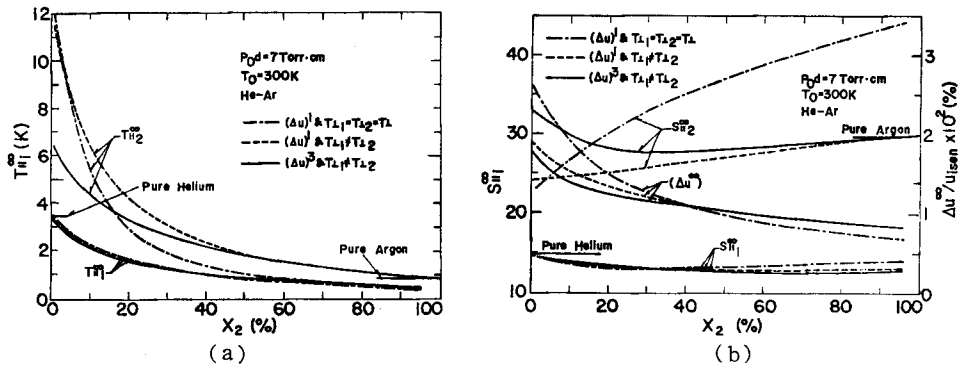


Fig. 4. Dependencies of (a) frozen parallel temperature of each species, (b) terminal speed ratio of each species and terminal velocity slip on mole fraction of heavy species, χ_2 , for an He-Ar mixture calculated at $P_0 d = 7$ Torr·cm and $T_0 = 300$ K for three cases.

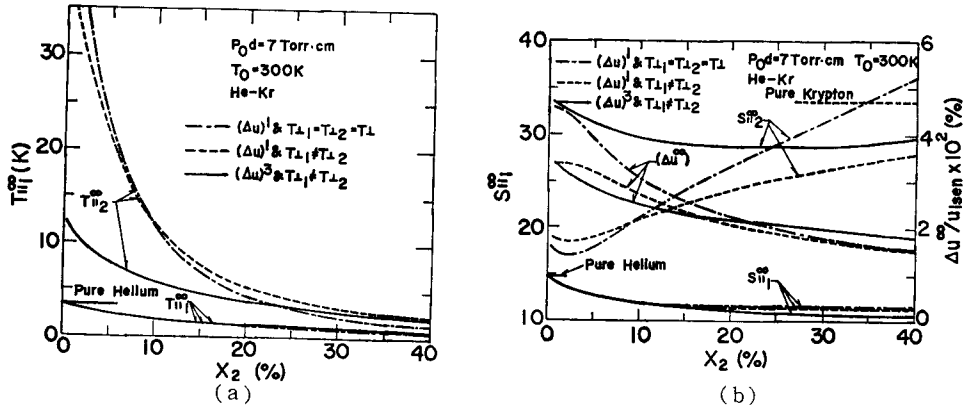


Fig. 5. Dependencies of (a) frozen parallel temperature of each species, (b) terminal speed ratio of each species and terminal velocity slip on mole fraction of heavy species, χ_2 , for an He-Kr mixture calculated at $P_0 d = 7$ Torr·cm and $T_0 = 300$ K for three cases.

is always higher than that of the light species for all cases. This result qualitatively agrees with Miller and Andres' theoretical calculation,⁵⁾ and Cooper and Bienkowski's theory⁷⁾ and Chatwani and Fiebig's Monte-Carlo result.⁹⁾ With an increase of χ_2 the collision frequency between the light-light species decreases, while those between the light-heavy and heavy-heavy species increase. Because of the increase in the collision frequencies between the light-heavy and heavy-heavy species, both $T_{i_1}^\infty$ and $T_{i_2}^\infty$ decrease with χ_2 as shown in Figs. 3(a), 4(a), and 5(a). The frozen temperature of the light species shows no prominent dependency on the approximation of the velocity slip and the assumption of the perpendicular temperature, except for the case of the He-Ne mixture in $\chi_2 > 20\%$, while the frozen temperature of the heavy species shows a prominent dependency on them. For the case of $T_{\perp_1} = T_{\perp_2} = T_\perp$ using $(\Delta u)^1$, $T_{i_2}^\infty$ rapidly approaches $T_{i_1}^\infty$ with χ_2 and does not approach the value of the pure heavy species. On the other hand, $T_{i_2}^\infty$ for $T_{\perp_1} \neq T_{\perp_2}$ using $(\Delta u)^3$ approaches the value of the pure heavy species and the ratio of $T_{i_2}^\infty/T_{i_1}^\infty$ shows a weak dependency on χ_2 . In the smaller range of χ_2 , its ratio gradually increases with χ_2 and has a maximum at some value of χ_2 . It decreases in the larger range of χ_2 for the He-Ne and He-Ar mixtures, while it always decreases with χ_2 for the He-Kr mixture: $T_{i_2}^\infty/T_{i_1}^\infty = 1.68$ at $\chi_2 = 1\%$, 1.94 at 40% and 1.69 at 90% for He-Ne, 1.94 at 1%, 2.17 at 20% and 1.80 at 90% for He-Ar, and 3.54 at 1%, 2.61 at 40% for He-Kr. The result whereby the dependency of $T_{i_2}^\infty/T_{i_1}^\infty$ on χ_2 for the He-Kr mixture is different from those for the He-Ne and He-Ar mixtures means that the velocity slip for the He-Kr mixture is not sufficiently small enough to neglect the fourth and higher order terms of the velocity slip in the calculation of the collision terms between the different species. Campargue *et. al.*²⁾ have obtained the value of 2.2 at $\chi_2 = 1\%$ and 2.46 at 5% for the He-Ar mixture by the molecular beam time-of-flight measurements. Although the present results are slightly smaller than their experimental results, qualitatively good agreement in the dependency of the ratio of $T_{i_2}^\infty/T_{i_1}^\infty$ on χ_2 between them is obtained for the case of $T_{\perp_1} \neq T_{\perp_2}$ using $(\Delta u)^3$. They also have obtained the ratio of $T_{i_2}^\infty/T_{i_1}^\infty$ for several gas mixtures: 2-2.5 for He-Ar ($m_2/m_1 \cong 10$), 4-4.5 for He-Xe ($m_2/m_1 \cong 33$) and 13-15 for H₂-Xe ($m_2/m_1 \cong 65$). The present results qualitatively explain the dependency of $T_{i_2}^\infty/T_{i_1}^\infty$ on the mass ratio. The frozen parallel temperature of the heavy species for $T_{\perp_1} \neq T_{\perp_2}$ using $(\Delta u)^1$ is almost equal to that for $T_{\perp_1} = T_{\perp_2} = T_\perp$ using $(\Delta u)^1$ in the smaller range of χ_2 for the He-Ar and He-Kr mixtures, but approaches the value for $T_{\perp_1} \neq T_{\perp_2}$ using $(\Delta u)^3$ with χ_2 for all cases of mixtures. This result means that the discrepancy between $T_{i_2}^\infty$ for the $(\Delta u)^1$ and $(\Delta u)^3$ approximations in the smaller range of χ_2 is mainly due to the truncation error of the velocity slip in the calculation of the collision terms. The discrepancy between those for $T_{\perp_1} = T_{\perp_2} = T_\perp$ and $T_{\perp_1} \neq T_{\perp_2}$ in the

larger range of χ_2 is mainly due to the summation of $A_{22}[v_{\perp 2}^2]$ and $A_{21}[v_{\perp 2}^2]$ determined from Eq. (3.12) and that calculated from Eqs. (3.5) and (3.32).

Assuming equal perpendicular temperatures, the present results give the physical contradiction that the parallel temperature of the heavy species does not approach the value of pure heavy species. However, by neglecting Eq. (3.12) and by evaluating the collision term between the heavy-heavy species from Eq. (3.32), this contradiction can be avoided. This fact means that we should consider the translational non-equilibrium not only between the parallel temperatures of the light and heavy species but also between their perpendicular temperatures in the translational relaxation process of the binary gas mixture. Nevertheless, this assumption has no apparent effect on the result for $T_{\parallel 1}^{\infty}$ in a wide range of χ_2 and their mass ratio. Furthermore, it has only a weak effect on the result for $T_{\parallel 2}^{\infty}$ in the smaller range of χ_2 and for the larger mass ratio, where we should include the higher order terms of the velocity slip in the calculation of the collision terms.

Although $T_{\parallel 2}^{\infty}$ is higher than $T_{\parallel 1}^{\infty}$, the terminal speed ratio of the heavy species is always larger than that of the light species for all cases. That of the light species has a weak dependency on the approximation of the velocity slip and the assumption of the equal perpendicular temperatures, and gradually decreases with χ_2 from the value of the pure light species. However, $S_{\parallel 2}^{\infty}$ shows a strong dependency on them because of the dependency of $T_{\parallel 2}^{\infty}$ on them. The terminal speed ratio of the heavy species for $T_{\perp 1} = T_{\perp 2} = T_{\perp}$ using $(\Delta u)^1$ rapidly increases with χ_2 , and becomes much larger than the value of the pure heavy species. However, $S_{\parallel 2}^{\infty}$ for $T_{\perp 1} \neq T_{\perp 2}$ using $(\Delta u)^3$ decreases with χ_2 : for the He-Ne mixture it decreases with χ_2 and approaches the value of pure neon, but for the He-Ar and He-Kr mixtures it decreases with χ_2 and has a minimum at some value of χ_2 and increases to approach the value of the pure heavy species. It can be also seen that $S_{\parallel 2}^{\infty}$ for $T_{\perp 1} \neq T_{\perp 2}$ using $(\Delta u)^3$ in the smaller range of χ_2 is larger than the value of pure heavy species for the He-Ne and He-Ar mixtures. These results qualitatively agree with the experiments of Campargue *et. al.*,²⁾ who found that $S_{\parallel 2}^{\infty}$ decreases with χ_2 and $S_{\parallel 2}^{\infty}$ is larger than the value of the pure heavy species in the smaller range of χ_2 . For $T_{\perp 1} \neq T_{\perp 2}$ using $(\Delta u)^1$, $S_{\parallel 2}^{\infty}$ decreases with χ_2 for the He-Ne mixture, but increases for the He-Ar and He-Kr mixtures, and approaches that for $T_{\perp 1} \neq T_{\perp 2}$ using $(\Delta u)^3$.

The stream velocity of the light species is larger than that of the heavy species, and the terminal velocity slip increases with a decrease of χ_2 and an increase of the mass ratio for all the cases. The terminal velocity slip for $T_{\perp 1} = T_{\perp 2} = T_{\perp}$ using $(\Delta u)^1$ shows the strongest dependency on χ_2 of the three cases, while that for $T_{\perp 1} \neq T_{\perp 2}$ using $(\Delta u)^3$ shows the weakest dependency of them. The terminal velocity slip for $T_{\perp 1} \neq T_{\perp 2}$

using $(\Delta u)^1$ almost agrees with Δu^∞ for $T_{\perp 1} \neq T_{\perp 2}$ using $(\Delta u)^3$ in the cases of the He-Ne and He-Ar mixtures, but approaches that for $T_{\perp 1} = T_{\perp 2} = T_{\perp}$ using $(\Delta u)^1$ with χ_2 in the case of the He-Kr mixtures. This discrepancy is also due to the truncation error of the velocity slip in the calculation of the collision terms because of the larger velocity slip between helium and krypton.

Dependencies of the terminal speed ratio of each species and the terminal velocity slip on $P_0 d$ calculated at $\chi_2 = 3\%$ and $T_0 = 300$ K are shown in Figs. 6-8 for the He-Ne, He-Ar and He-Kr mixtures, respectively. It can be seen that S_{i1}^∞ , S_{i2}^∞ and Δu^∞ show an exponential dependency on $P_0 d$, except for the smaller range of $P_0 d$, where non-equilibrium effects may exist upstream from the starting point and further the velocity slip may become larger in the expansion to make the assumption of the isentropic expansion to the starting point and the very small velocity slip invalid. The terminal speed ratio of the light species shows no apparent dependency on the approximation of the velocity slip and the assumption of the equal perpendicular temperatures, while S_{i2}^∞ shows a strong dependency on them. For the $(\Delta u)^1$ approx-

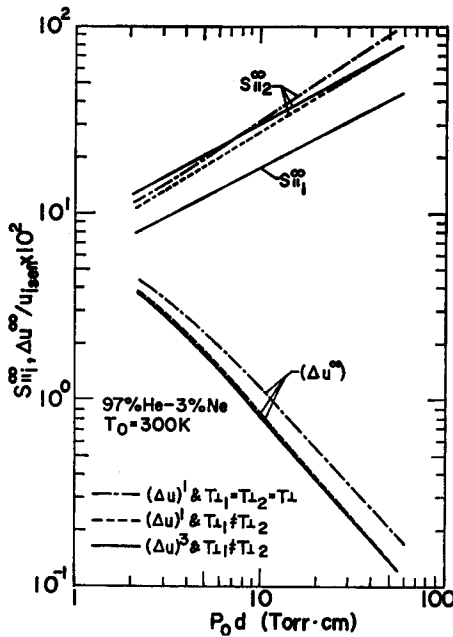


Fig. 6. Dependencies of terminal speed ratio of each species and terminal velocity slip on $P_0 d$ for a 97% He-3% Ne mixture calculated at $T_0 = 300$ K for three cases: (i) $T_{\perp 1} = T_{\perp 2} = T_{\perp}$ using the $(\Delta u)^1$ approximation. (ii) $T_{\perp 1} \neq T_{\perp 2}$ using $(\Delta u)^1$ and (iii) $T_{\perp 1} \neq T_{\perp 2}$ using $(\Delta u)^3$.

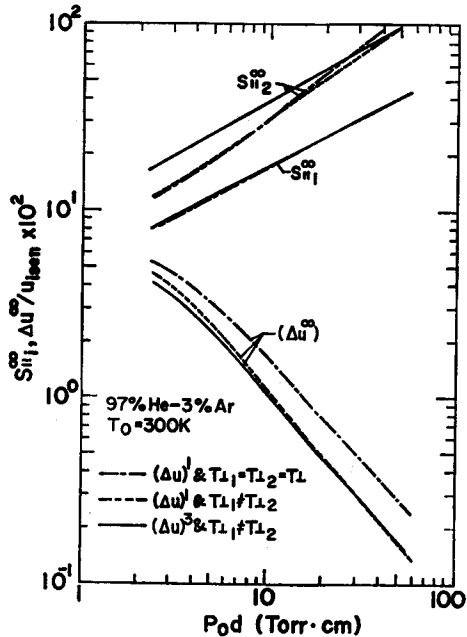


Fig. 7. Dependencies of terminal speed ratio of each species and terminal velocity slip on $P_0 d$ for a 97% He-3% Ar mixture calculated at $T_0 = 300$ K for three cases.

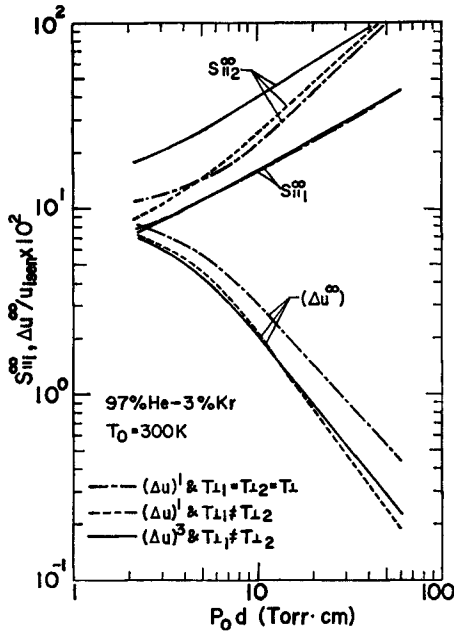


Fig. 8. Dependencies of terminal speed ratio of each species and terminal velocity slip on $P_0 d$ for a 97% He-3% Kr mixture calculated at $T_0 = 300$ K for three cases.

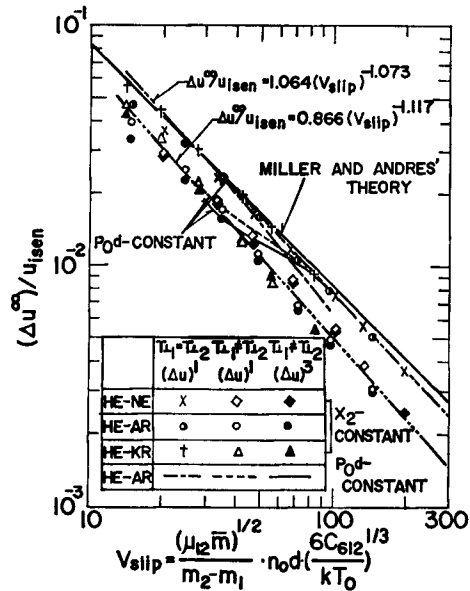


Fig. 9. Correlation of calculated velocity slip with the Miller and Andres slip parameter⁵ together with their theoretical prediction.

ximation, the ratio of $S_{ii}^{\infty}/S_{ii}^{\infty}$ shows a prominent dependency on $P_0 d$ and its variation is different depending on the extent of the velocity slip. On the other hand, its ratio for $T_{L1} \neq T_{L2}$ using $(\Delta u)^3$ shows a weak dependency on $P_0 d$: 1.64-1.75 for He-Ne, 2.14-2.32 for He-Ar and 2.33-2.73 for He-Kr against $P_0 d = 3-30$ Torr·cm. This result also means that the calculated result for the $(\Delta u)^1$ approximation is influenced by the truncation error of the velocity slip. The terminal velocity slip calculated for $T_{L1} = T_{L2} = T_L$ using $(\Delta u)^1$ is the largest of the three cases, while that for $T_{L1} \neq T_{L2}$ using $(\Delta u)^1$ agrees with Δu^{∞} for $T_{L1} \neq T_{L2}$ using $(\Delta u)^3$ in the case of the He-Ne mixture, and shows a slightly stronger dependency on $P_0 d$ than that in the case of the He-Ar and He-Kr mixtures because of the increase in the velocity slip.

The terminal velocity slips calculated at $\chi_2 = 3\%$ and $T_0 = 300$ K for a χ_2 -constant and at $P_0 d = 7$ Torr·cm and $T_0 = 300$ K for a $P_0 d$ -constant (only in the case of the He-Ar mixture) are plotted against a slip parameter, V_{slip} , introduced by Miller and Andres⁵ in Fig. 9, together with their theoretical prediction. In the slip parameter, \bar{m} is the average mass of the mixture, and C_{612} is the coefficient of the attractive term in the Lennard-Jones (12, 6) potential between the light and heavy species given in Eq. (3.13). It can be seen that Δu^{∞} calculated for the χ_2 -constant has a good correlation with the V_{slip} , while Δu^{∞} calculated for the $P_0 d$ -constant has the same correlation

with the V_{slip} as that for the χ_2 -constant in the much smaller range of χ_2 , but deviates from its correlation with an increase of χ_2 . The terminal velocity slip calculated for the χ_2 -constant for $T_{\perp 1}=T_{\perp 2}=T_{\perp}$ using $(\Delta u)^1$ is in good agreement with the Miller and Andres theoretical prediction, but those for $T_{\perp 1} \neq T_{\perp 2}$ are smaller than their theoretical prediction. From this figure, we can find the following relations between the terminal velocity slip and the Miller and Andres slip parameter in the range of χ_2 less by about 8%:

$$\Delta u^{\infty}/u_{ism} = 1.064(V_{slip})^{-1.073} \text{ for } T_{\perp 1}=T_{\perp 2}=T_{\perp} \text{ using } (\Delta u)^1,$$

$$\Delta u^{\infty}/u_{ism} = 0.866(V_{slip})^{-1.117} \text{ for } T_{\perp 1} \neq T_{\perp 2} \text{ using } (\Delta u)^1 \text{ and } (\Delta u)^3.$$

The reduced frozen parallel temperatures of the light and heavy species calculated at $\chi_2=3\%$ and $T_0=300\text{ K}$ for a χ_2 -constant and at $P_0d=7\text{ Torr}\cdot\text{cm}$ and $T_0=300\text{ K}$ for a P_0d -constant (only in the case of the He-Ar mixture) are plotted against a frozen temperature parameter of Patch⁴⁾, T_{patch} , in Fig. 10(a) and (b). Patch's frozen temperature parameter is a complicated function of the reservoir density, mass ratio, mole fraction and potential parameters presented in Eqs. (46)–(50) of Ref. 4. In his parameter, (m_i/m_j+5) in Eq. (47) must be replaced with $(m_i/m_j+5\Omega_{ij}(1,1)^*/2\Omega_{ij}(2,2)^*)$, where $\Omega_{ij}(1,1)^*$ and $\Omega_{ij}(2,2)^*$ are the standard collision integrals which occurred in the Chapman-Enskog expression for binary diffusion and viscosity, respectively.¹⁶⁾ It can be seen that T_{ii}^{∞} has a good correlation with its scaling parameter independent of the approximation of the velocity slip and the assumption of the

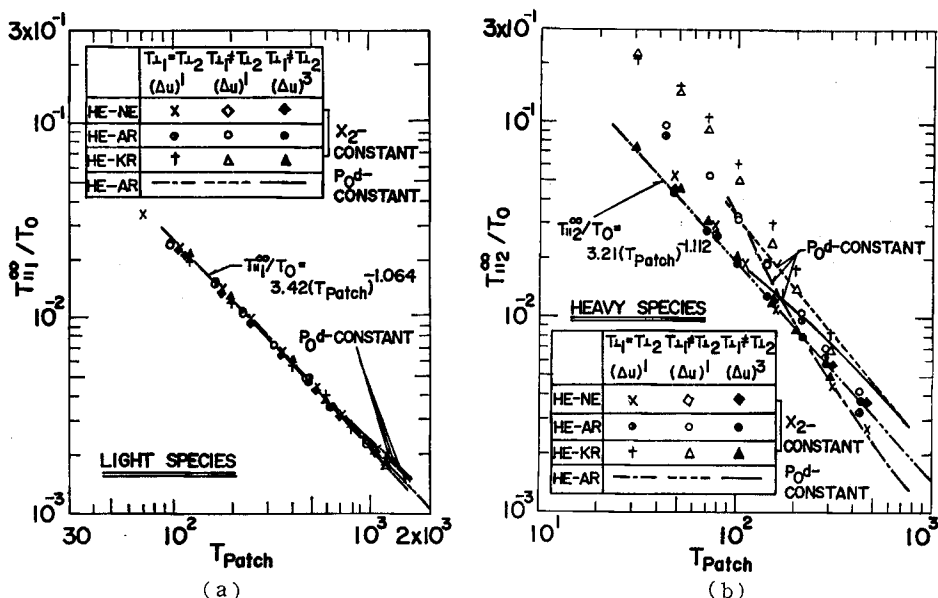


Fig. 10. Correlations of calculated frozen parallel temperatures of (a) light and (b) heavy species with Patch's frozen temperature parameter.⁴⁾

equal perpendicular temperatures, except for the much larger value of χ_2 in the case of the P_0d -constant. On the other hand, $T_{\parallel 2}^\infty$ has a dependency not only on them but also on the mass ratio. Only in the case of $T_{\perp 1} \neq T_{\perp 2}$ using the $(\Delta u)^3$ approximation, $T_{\parallel 2}^\infty$ calculated for the χ_2 -constant has a good correlation with Patch's frozen temperature parameter. $T_{\parallel 2}^\infty$ for the P_0d -constant has the same correlation with that for the χ_2 -constant in the much smaller range of χ_2 , but deviates from its correlation with an increase of χ_2 . From these figures, we can find the following relations between the frozen temperatures of the light and heavy species and Patch's frozen temperature parameter as follows:

(i) for light species,

$$T_{\parallel 1}^\infty = 3.42(T_{Patch})^{-1.064},$$

(ii) for heavy species in the range of χ_2 less by about 5%,

$$T_{\parallel 2}^\infty = 3.21(T_{Patch})^{-1.112} \text{ for } T_{\perp 1} \neq T_{\perp 2} \text{ using } (\Delta u)^3.$$

6. Conclusions

By assuming the ellipsoidal velocity distribution function as the velocity distribution function of gas molecules, we could consider the realistic inter-molecular potential model in the evaluation of the collision terms. Furthermore, by assuming equal perpendicular temperatures and a very small velocity slip, we could replace the sixth-order multiple integral to an infinite series of multiplications of four single integrals in the calculation of the collision terms between light and heavy species. Also, we could numerically analyze the problem of the translational non-equilibrium and the velocity slip in the spherically symmetrical expansion of the binary gas mixture. Although the assumption of the equal perpendicular temperatures seems physically unrealistic, its effect on the results for $T_{\parallel 1}^\infty$ is very small and the effect on the results for $T_{\parallel 2}^\infty$ becomes smaller with an increase of the mass ratio, m_2/m_1 , and a decrease of the mole fraction of the heavy species, χ_2 . On the other hand, the truncation error of the velocity slip in the calculation of the collision terms has no apparent effect on the results for $T_{\parallel 1}^\infty$, but has a larger effect on the results for $T_{\parallel 2}^\infty$ with an increased m_2/m_1 and a decreased χ_2 . From the present results, we have obtained the following conclusions:

- 1) The frozen parallel temperature of the heavy species is higher than that of the light species, and the ratio of $T_{\parallel 2}^\infty/T_{\parallel 1}^\infty$ increases with an increase of m_2/m_1 .
- 2) The stream velocity of the heavy species is smaller than that of the light species, and the terminal velocity slip increases with an increase of m_2/m_1 and a decrease of P_0d and χ_2 .
- 3) The terminal speed ratio of the heavy species is larger than that of the light species, and the ratio of $S_{\parallel 2}^\infty/S_{\parallel 1}^\infty$ increases with m_2/m_1 .

These results qualitatively explain the previously obtained experimental results.

References

- 1) Abuaf, N., Anderson, J. B., Andres, Fenn, J. B., and Miller, D. R., "Studies of Low Density Supersonic Jets," *Proc. 5th Int. Symp. on Rarefied Gas Dynamics*, Vol. II, edited by C. Brundin, Academic Press, New York, 1967, pp. 1317-1336.
- 2) Campargue, R., Lebéhot, A., Lemonnier, J. C., and Marette, D., "Measured, Very Narrow Velocity Distributions for Heated, Xe and Ar-Seeded Nozzle-Type Molecular Beams of He and H₂ Skimmed from Freejets Zones of Silence; Xe Energies up to 30eV," *Proc. 12th Int. Symp. on Rarefied Gas Dynamics*, Vol. 74, Part II, edited by S. S. Fisher, AIAA, New York, 1981, pp. 823-843.
- 3) Anderson, J. B., "Intermediate Energy Molecular Beams from Freejets of Mixed Gases," *Entropie*, Vol. 18, 1967, pp. 33-37.
- 4) Patch, D. F., "Application of Free Jet Sources to Reactive Crossed Molecular Beam Experiments," Ph. D. Dissertation, University of California, San Diego, 1972.
- 5) Miller, D. R., and Andres, R. P., "Translational Relaxation in Low Density Supersonic Jets," *Proc. 6th Int. Symp. on Rarefied Gas Dynamics*, Vol. II, edited by L. Trilling and H. V. Wachman, Academic Press, New York, 1969, pp. 1385-1402.
- 6) Willis, D. R., and Hamel, B. B., "Non-Equilibrium in Spherical Expansion of Polyatomic Gases and Gas Mixtures," *Proc. 5th Int. Symp. on Rarefied Gas Dynamics*, Vol. I, edited by C. Brundin, Academic Press, New York, 1967, pp. 837-860.
- 7) Cooper, A. L., and Bienkowski, G. K., "An Asymptotic Theory for Steady Source Expansion of a Binary Gas Mixture," *Proc. 5th Int. Symp. on Rarefied Gas Dynamics*, Vol. I, edited by C. Brundin, Academic Press, New York, 1967, pp. 861-879.
- 8) Soga, T., and Oguchi, H., "Source Flow Expansion of Gas Mixtures into a Vacuum," *Proc. 9th Int. Symp. on Rarefied Gas Dynamics*, Vol. I, edited by M. Becker and M. Fiebig, DFVLR Press, Porz-Wahn, 1974, pp. B. 3-1~B. 3-9.
- 9) Chatwani, A. U., and Fiebig, M., "Source Expansion of Monatomic Gas Mixtures," *Proc. 12th Int. Symp. on Rarefied Gas Dynamics*, Vol. 74, Part II, edited by S. S. Fisher, AIAA, New York, 1981, pp. 785-801.
- 10) Knuth, E. L., and Fisher, S. S., "Low-Temperature Viscosity Cross Sections Measured in a Supersonic Argon Beam," *The Journal of Chemical Physics*, Vol. 48, 1968, pp. 1674-1684.
- 11) Toennies, J. P., and Winkelmann, K., "Theoretical Studies of Highly Expanded Free Jets: Influence of Quantum Effects and a Realistic Intermolecular Potential," *The Journal of Chemical Physics*, Vol. 66, 1977, pp. 3965-3979.
- 12) Brusdeylins, G., Meyer, H. D., Toennies, J. P., and Winkelmann, K., "Production of Helium Nozzle Beams with Very High Speed Ratios," *Proc. 10th Int. Symp. on Rarefied Gas Dynamics*, Part II, edited by J. L. Potter, AIAA, New York, 1977, pp. 1047-1059.
- 13) Campargue, R., Lebéhot, A., and Lemonnier, J. C., "Nozzle Beam Speed Ratios above 300 Skimmed in a Zone of Silence of He Freejets," *Proc. 10th Int. Symp. on Rarefied Gas Dynamics*, Part II, edited by J. L. Potter, AIAA, New York, 1977, pp. 1033-1046.
- 14) Vincenti, W. G., and Kruger, Jr., C. H., "Introduction to Physical Gas Dynamics," John Wiley and Sons, New York, 1965, Chap. 9.
- 15) Hirschfelder, J. O., Bird, R. B., and Spotz, E. L., "The Transport Properties for Non-Polar Gases," *The Journal of Chemical Physics*, Vol. 16, 1948, pp. 968-981.
- 16) Hirschfelder, J. O., Curtiss, C. F., and Bird, R. B., "Molecular Theory of Gases and Liquids," John Wiley and Sons, New York, 1954, Chap. 8.
- 17) Tang, K. T., and Toennies, J. P., "A simple theoretical model for the van der Waals potential at intermediate distances. I. Spherically symmetric potentials," *The Journal of Chemical Physics*, Vol. 66, 1977, pp. 1496-1506; Erratum, Vol. 67, 1977, p. 375.
- 18) Ashkenas, H., and Sherman, F. S., "The Structure and Utilization of Supersonic Free Jets in Low Density Wind Tunnel," *Proc. 4th Int. Symp. on Rarefied Gas Dynamics*, Vol. II, edited by J. H. de Leeuw, Academic Press, New York, 1965, pp. 84-105.